The CBC microstrip readout chip for CMS at the High Luminosity LHC

2012 JINST 7 C08006

(http://iopscience.iop.org/1748-0221/7/08/C08006)

PUBLISHED BY IOP PUBLISHING FOR SISSA MEDIALAB

RECEIVED: *June 11, 2012*
ACCEPTED: *July 23, 2012*
PUBLISHED: *August 28, 2012*

WIT2012 — WORKSHOP ON INTELLIGENT TRACKERS,
3–5 MAY 2012,
INFN PISA, ITALY

The CBC microstrip readout chip for CMS at the High Luminosity LHC

W. Ferguson,[a,1] D. Braga,[a,b] J. Fulcher,[a] G. Hall,[a] J. Jacob,[c] L. Jones,[b] M. Pesaresi,[a] M. Prydderch[b] and M. Raymond[a]

[a] *Blackett Laboratory, Imperial College, London, SW7 2AZ, U.K.*
[b] *Rutherford Appleton Laboratory, Didcot, OX11 0QX, U.K.*
[c] *HH Wills Laboratory, Bristol, Bristol, BS8 1TL, U.K.*

E-mail: william.ferguson02@imperial.ac.uk

ABSTRACT: The CMS Binary Chip (CBC) is designed for readout of silicon microstrips in the CMS Tracker at the High Luminosity LHC (HL-LHC). Binary, unsparsified readout is well suited to the high luminosity environment, where particle fluences and data rates will be much higher than at the LHC. In September 2011, a module comprising a CBC bonded to a silicon microstrip sensor was tested with 400 GeV protons in the H8 beamline at CERN. Performance was in agreement with expectations. The spatial resolution of the sensor and CBC has been shown to be better than pitch/$\sqrt{12}$ due to spatial distribution of one and two strip clusters. Large cluster events show consistency with the production of delta rays. At operating thresholds, the hit efficiency has been shown to be approximately 98%, limited by the resolution of timing apparatus, while the noise occupancy is measured to be below 10^{-4}. The distribution of charge deposition in the sensor has been reconstructed by measurement of the hit efficiency as a function of comparator threshold; assuming the underlying distribution is a Landau.

KEYWORDS: Electronic detector readout concepts (solid-state); Front-end electronics for detector readout

[1] Corresponding author.

doi:10.1088/1748-0221/7/08/C08006

2012 JINST 7 C08006

Contents

1 Introduction

The High Luminosity LHC (HL-LHC) foresees an order of magnitude increase in luminosity towards 5x10^{34} cm^{-2}s^{-1} with the principal aim of increasing statistics in order to significantly extend the physics reach of the LHC.

The increase in luminosity does however have serious implications for the CMS Silicon Strip Tracker (SST). The increased particle fluence will necessitate the complete replacement of the tracker before 2022 due to accumulated radiation damage of the sensors and potentially intolerable detector occupancies. The replacement tracker must have higher granularity, leading to increased power consumption and hence cooling requirements and material. In addition, the first level trigger rate must remain below 100 kHz in order to maintain compatibility with existing systems, and will for the first time require information from the tracker.

Readout of the silicon microstrips is currently performed by the APV25 [1], which is an analogue, un-sparsified chip, fabricated in 0.25 μm CMOS. However, such a system will not be possible at the HL-LHC. Digital off-detector links will be used, which require on chip digitisation of pulse height information, and sparsification to keep data rates manageable. This would lead to a complicated chip, with large power consumption.

The implementation of a binary, unsparsified architecture has therefore been proposed, which will maintain chip simplicity, at the cost of pulse height information. The CMS Binary Chip (CBC) is a prototype readout chip for short strips in the upgraded CMS strip tracker.

2 CMS Binary Chip

The CBC is a 128 channel wire-bonded chip fabricated in 130 nm CMOS. The front end input pads are in two staggered rows, with an effective pitch of 50 μm. The sensor can be DC or AC coupled to the front-end preamplifier, and can be selected to read either electrons or holes. The analogue pulse shape has an overall peaking time of 20 ns following the post-amplification stage with a gain of $\sim$50 mVfC^{-1}. Channel to channel DC shifts can be corrected via programmable offsets before the pulse is compared against a global programmable threshold at the comparator, and sampled into pipeline memory at 40 MHz. The pipeline RAM is 256 samples deep, which corresponds to a 6.4 μs latency for the first level trigger.

The amplifier noise depends on the external capacitance added at the preamplifier input, and has been shown to vary approximately as 500 + 64 C_{ext}/pF rms electrons, where C_{ext} is the external capacitance [2]. This dependence is the same for both electron and holes. The preamplifier current is increased with external capacitance in order to maintain the pulse shape, which leads to a dependence of analogue power on external capacitance. Including digital power consumption of <50 μW/channel, the total power is given by 180 + 21 C_{ext}/pF, in μW per channel [2].

Upon a trigger, the 128 bits of data stored in the pipeline one latency period before are retrieved and stored in a readout buffer. The buffer can accommodate up to 32 triggered data sets awaiting readout, and has a width of 136 bits, which corresponds to the 128 channels and an 8 bit pipeline address. Further details on specifications and the design of the front-end circuitry and its performance can be found in [2].

3 Beam tests in H8

The CBC was tested with 400 GeV protons at the CERN H8 beamline in September 2011, with a CBC module being operated parasitically in the UA9 test beam (figure 2). The UA9 collaboration investigates the phenomenon of crystal channeling, where a bent crystal is used to bend charged particle trajectories [3]. A telescope with excellent spatial and angular resolution has been used for measuring such trajectories [4], and thus provided a good platform on which to test the CBC module in the presence of a well characterised beam.

3.1 CBC module

A single CBC was used to read out a 5 cm long p-on-n silicon strip sensor. The sensor was fan shaped with pitch varying from 120–150 μm, and thickness 320 μm. The 64 strips of the sensor were bonded to alternate CBC channels. Control and readout were performed by an FPGA based VME DAQ card called the CiDAQ (section 3.3).

3.2 Telescope

The telescope consisted of ten silicon microstrip sensors, arranged as five planes of orthogonal sensor pairs, to give five two-dimensional hit positions along the beamline. Two planes were placed upstream of the crystal, and two downstream, with a third downstream plane rotated by 45° to resolve hit ambiguities from multiple tracks. Both upstream and downstream arms had a length of approximately 10 m. The layout of the telescope is shown in figure 2.

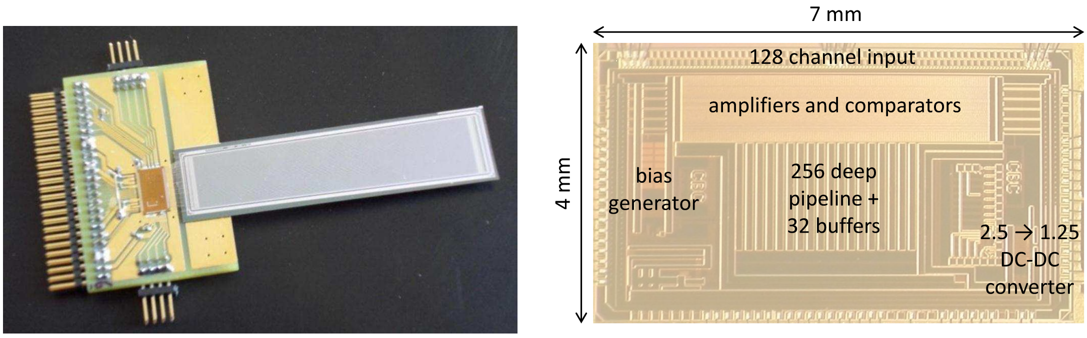

Figure 1. Left: the CBC chip and test board, wire-bonded to a 5 cm long sensor. Right: the CBC layout.

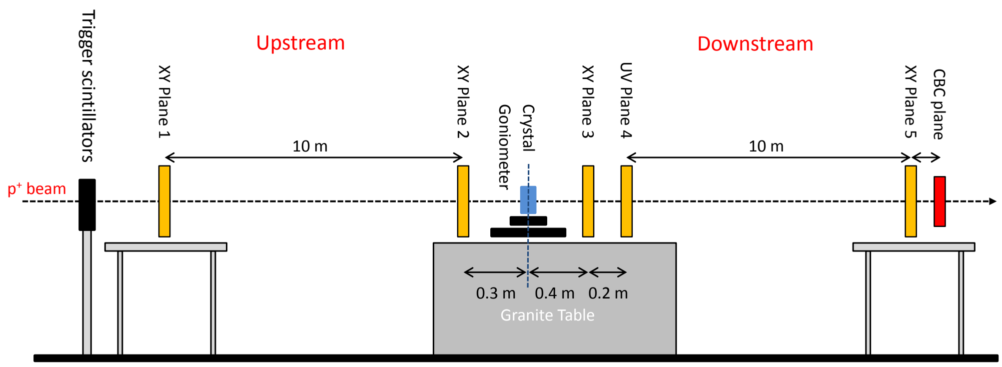

Figure 2. Telescope and CBC module layout in the H8 beamline. Distances are approximate.

The sensors are 320 μm thick and have 639 readout strips of 60 μm pitch, with intermediate floating strips, which improve charge sharing. The sensor readout is based on that of the CMS silicon microstrip tracker [5]. Strips are read out by the APV25, which is an analogue, 128 channel, 0.25 μm CMOS chip, specifically designed for the CMS tracker [6]. Each sensor has a front end hybrid with six APV25 chips which are multiplexed onto three output lines (only five chips are used to readout the 639 strips, one is unused). An analogue optical hybrid (AOH) [7] on each front end hybrid converts the three electrical signals to optical signals, which are transmitted on single mode optical fibres.

3.3 Data acquisition and reconstruction

The telescope DAQ used during this beam test is based on the system described in [4] and has been modified to accept data from the CBC module (figure 3). Changes include increase of the peak DAQ rate to 50 kHz and replacement of the trigger controller and sequencer boards with the CiDAQ; an FPGA based VME DAQ card that receives triggers, performs fast control of the telescope planes and CBC module, and reads out signals from the CBC module. The triggers are received from a scintillator upstream of the telescope. The CiDAQ provides a trigger timestamp resolution with <7 ns resolution and throttles the trigger, based on the APV25 buffer occupancies and the DAQ status from the CMS Front End Driver (FED). On receipt of a trigger, binary data

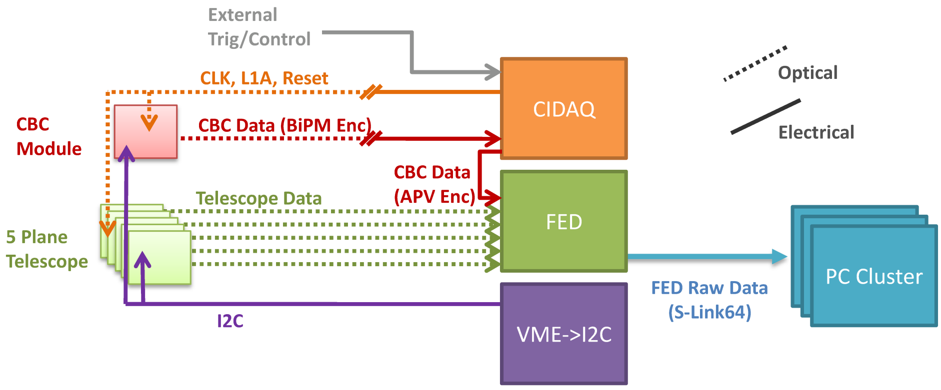

Figure 3. Schematic of the telescope and CBC module DAQ.

from all 128 channels are shifted out of the CBC at 40 MHz and are transmitted optically to the CiDAQ in the counting room.

In order to DC balance the optical link, the CBC data stream is encoded on module using a bi-phase mark line code scheme. The CiDAQ decodes and buffers the CBC data before it is retransmitted to the FED, in time with the APV25 data arriving from the telescope. In order to maintain compatibility with the telescope the CiDAQ encodes the CBC frames as APV25 frames. In this way, CBC data are event synchronised with the telescope and propagate through the high rate CMS-based online framework demonstrated in [4], where the event can be accessed online for monitoring and selection before storage to disk.

Details of hit reconstruction on the telescope planes are given in [4]. Track reconstruction can be performed in various ways depending on the requirements. For the purpose of evaluating the CBC module, only the downstream track is required, and this comes from a simple straight line fit to hits in the three downstream planes. The uncertainties in the track parameters come from the position resolution of the sensors and the contribution of multiple scattering from the sensors. Further details of track reconstruction are given in [4].

3.4 Telescope performance and selection cuts

The spatial resolution of each sensor has been measured to be 6.9 μm [4]. The angular resolution of the downstream track of the telescope depends on both the spatial resolution of the planes, and the effect of multiple scattering from the plane material, and has been estimated to be 2.7 urad [4]. The telescope was used to make event selection cuts, and to act as a comparison for the CBC data. The event selection cuts used were:

- one single downstream track in the telescope.
- track incident on CBC sensor (>2 mm from sensor edge).
- track incident within 3mm vertically of the nominal beam line, such that the pitch is effectively fixed at 134.4 μm.
- hit within 7 ns of sampling clock.

These selection cuts reduce the data volume by approximately 50%.

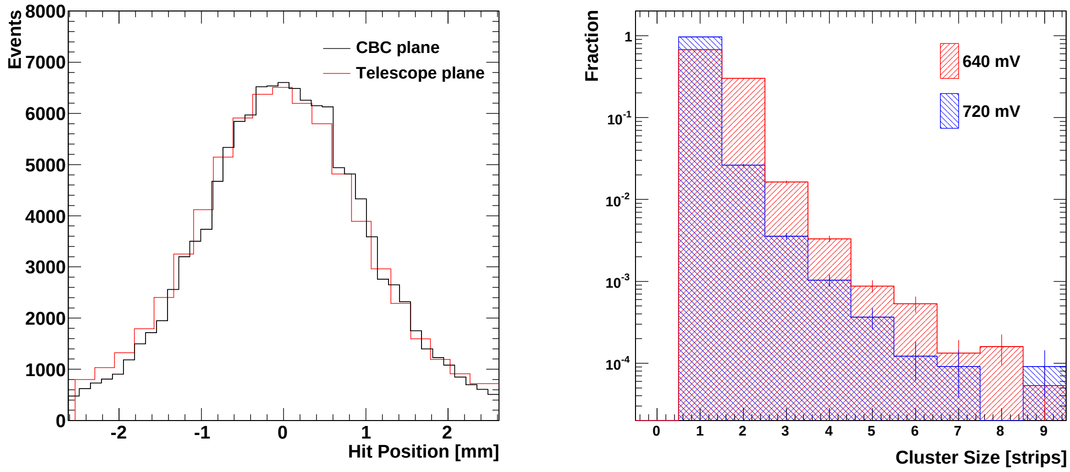

Figure 4. Left: beam profile in x for the 5^{th} telescope plane (units scaled) and the CBC sensor. Right: cluster size distributions for threshold voltages of 640 mV and 720 mV.

4 Results

Throughout the beam test over 30 million events were recorded and the CBC was found to operate as expected, with no pipeline errors and no CBC errors detected. Errors could have come from filling of the 32 bit buffer RAM, or the latency check circuit, which compares the difference in write and trigger counters to the programmed latency register. Preliminary tests have shown gain and noise to be uniform across channels.

Figure 4 shows a comparison of beam profiles from the CBC module and the 5^{th} telescope plane, and demonstrates good agreement. At a threshold of 720 mV there is a greater abundance of one strip clusters, in comparison to the distribution at the typical operating threshold of 640 mV, since only the strip with the highest charge in the cluster tends to exceed the threshold. Large cluster sizes of 3 or more strips can be attributed to rare, large charge deposition events, and delta electrons produced within the sensor material.

4.1 Spatial resolution

The spatial resolution of the CBC-sensor module is obtained from the residual distribution, with the residuals defined as the difference between extrapolated track position from the telescope, and the centre of the CBC cluster. The strip pitch at the nominal beam position was calculated iteratively as the value which minimised the spread of the residuals, and was found to be 134.4 μm. Due to the low beam divergence and scattering angle, and the close proximity of the CBC sensor to the last plane of the telescope, the extrapolated track position can simply be taken as the hit position in the last telescope plane. The spread in the residual distribution is then the quadrature sum of the resolution in the telescope plane and the resolution in the CBC module.

Figure 5 shows the distribution of residuals from one and two strip clusters, which make up 97.8% of all clusters, for all selected events (comparator threshold of 640 mV). Two strip clus-

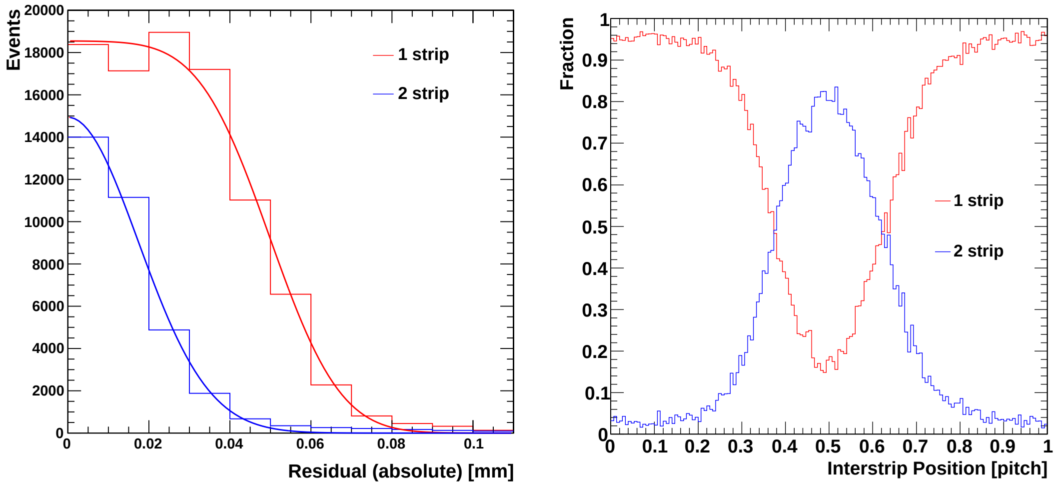

Figure 5. Left: absolute residual distributions for one and two strip clusters (threshold voltage 640 mV). A fit to the one strip cluster residuals gives a top-hat width of 99.6 μm and a Gaussian standard deviation of 13.8 μm. The combined spread of this distribution is 31.9 μm. The two strip cluster residuals are fitted with a Gaussian of width 17.4 μm. Right: proportion of all selected events that lead to one and two strip clusters as a function of interstrip position (0 and 1 correspond to the strip implant positions).

ters occur predominantly in a narrow region in between two adjacent strips, with one strip clusters dominating elsewhere. The distribution of one strip clusters is assumed to be a top-hat convoluted with a Gaussian which combines the indefinite boundary of the two regions with the telescope resolution. Subtracting out the contribution due to the telescope gives a CBC module resolution of 31.1 μm and 15.9 μm provided by one and two strip clusters respectively. The overall distribution, including clusters of $>$2 strips, is approximately Gaussian with standard deviation 30.2 μm. Accounting for the telescope resolution gives an overall CBC module resolution of 29.4 μm, which is better than the expected binary resolution of pitch / $\sqrt{12}$ due to the additional spatial information provided by the cluster size. Figure 5 also shows explicitly the relative proportion of one strip and two strip clusters across a strip.

4.1.1 Large cluster events

Figure 4 shows that one and two strip clusters dominate. However, clusters of four or more strips account for 0.5% of selected events and must therefore be understood. Large charge depositions corresponding to the high energy tail of the Landau distribution could explain clusters of up to a few strips wide, but larger clusters need an alternative explanation. Plots of residuals for 5 and 7 strip events are shown in figure 6. It is clear that each distribution shows two symmetric peaks about zero. Furthermore these peaks are separated by roughly the corresponding cluster width, indicating that the cluster is a result of a proton impact at one end of the cluster. One mechanism that could account for such events would be the production of delta rays along the proton path, propagating approximately transversely to the strip direction, creating a wide cluster. Residuals with intermediate values could be explained by events with multiple delta rays propagating in opposite directions.

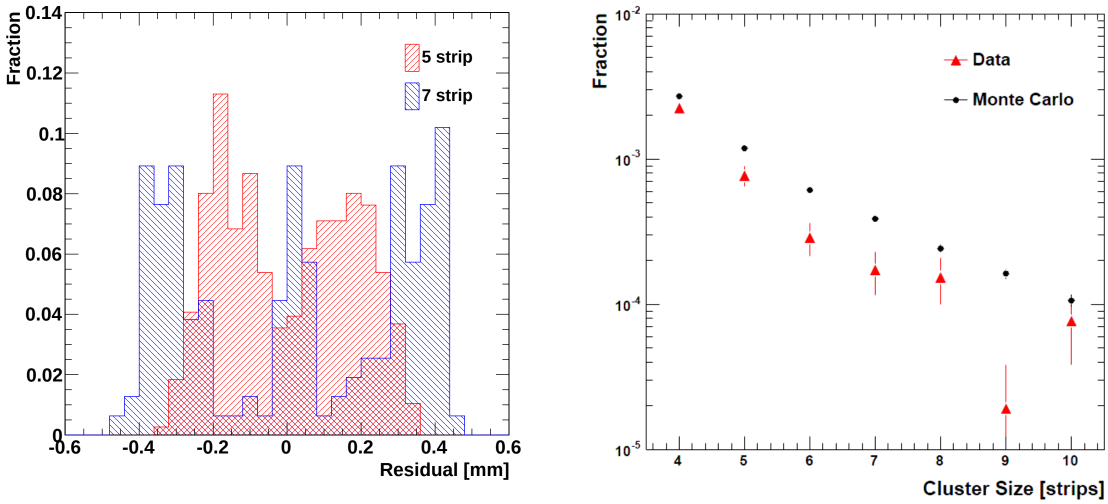

Figure 6. Left: normalised residuals for 5 strip clusters (761 events), and 7 strip clusters (157 events). Right: fraction of all clusters of size greater than three strips, shown for data (640 mV, only tracks incident within 0.2 pitch units of a strip selected) compared with Monte Carlo.

A simple Monte Carlo model was made to simulate the production of such events. The contribution from delta rays produced upstream is assumed to be negligible at the CBC position. Following the method outlined in [8], the probability distribution for producing a delta ray of certain energy per event is calculated for 400 GeV protons in 320 μm of silicon. The probability of producing a delta ray of certain energy scales approximately with the inverse square of this energy. A normalised probability distribution is then obtained by choosing an appropriate low energy cut off (143 keV). This distribution is sampled to produce a delta ray of certain energy for each event, at some random position along the path through the silicon, with isotropic distribution. The range of the delta electron is assumed to be a function of only energy, and follows the empirical formula given in [8]. Assuming linear energy loss along its path, the charge deposited in the final strip is calculated, and if greater than the threshold value set, the strip is included in the cluster. Figure 6 is the normalised cluster size distribution for the Monte Carlo model compared with data, for clusters of $>$3 strips. The Monte Carlo shows an excess of a factor of $\sim$2, although the general trends show good agreement.

The presence of these wide clusters would clearly have a detrimental effect on spatial resolution where the hit position is assumed to be the cluster centre. One method for overcoming this in a future tracker would be to monitor the residuals of wide clusters during reconstruction, and if the residual is half the cluster width, this could then be corrected for.

4.2 Noise occupancy and efficiency

The noise occupancy is measured by selecting only events where the track is incident outside of the CBC sensor region. This ensures that operating conditions are exactly the same as events with tracks incident on the CBC module. Figure 7 shows the variation of noise occupancy per bonded channel as a function of comparator threshold. The noise is seen to fall to around 10^{-4} at operating thresholds.

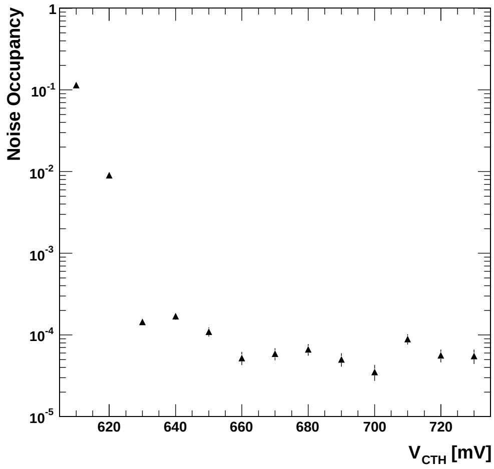

Figure 7. Noise occupancy per channel vs comparator threshold voltage (V_{CTH}).

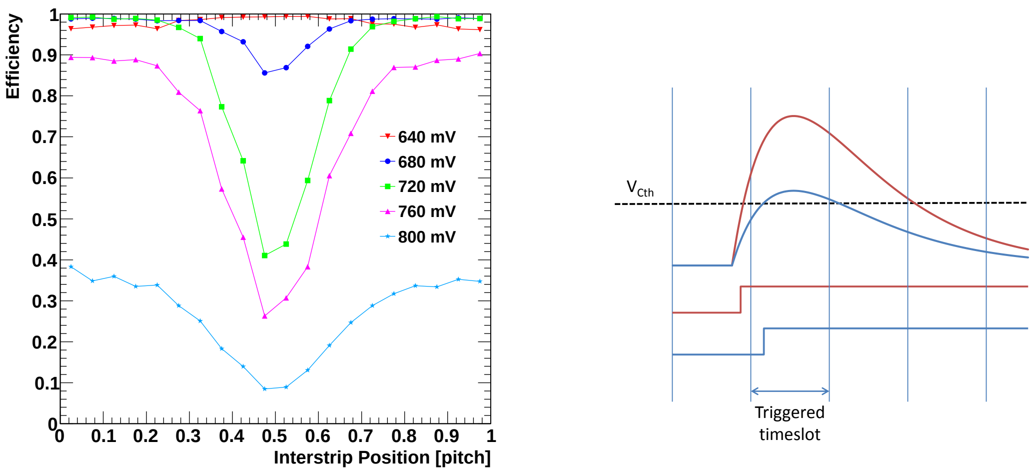

Figure 8. Left: efficiency as a function of inter-strip position in units of pitch (strip implants are at 0 and 1). Right: pulse shapes for large and small signals. Large signals could be missed if they fire the comparator before the triggered timeslot.

Efficiency is defined here as the proportion of selected events in the telescope that result in any hit in the CBC module. Figure 8 shows efficiency as a function of inter-strip position for various threshold voltages.

In the mid-strip region charge sharing between adjacent strips is increased, which leads to lower signals in these strips and a corresponding reduction in efficiency. This effect is greater at higher thresholds, as expected. At the operating threshold of 640 mV, the average efficiency is 98% but clearly dips near the strip implant regions. This can be explained by considering signals from single strip cluster events, which tend to occur around the strip implants (figure 5). For a

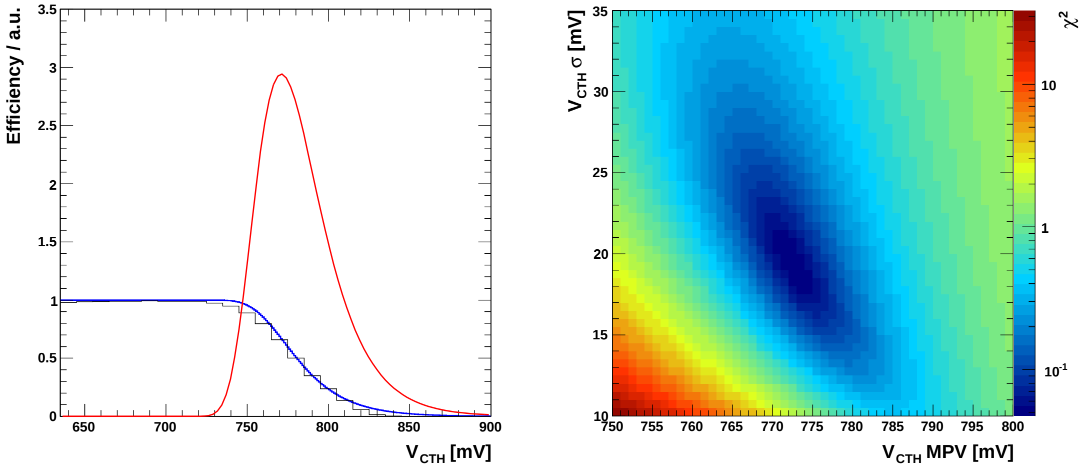

Figure 9. Left: efficiency as a function of threshold voltage for all events with hits expected within 20% pitch of a strip implant. The Landau distribution (red) comes from fitting its reverse integral (blue) to the data. The Landau distribution is scaled for clarity. Right: chi-squared distribution of the two free parameters, threshold MPV and σ.

1 fC threshold, the timewalk of the CBC has been found to be less than 16 ns for signals between 1.25 fC and 10 fC [2]. Since signals from single strip clusters tend to be larger (because charge is not shared), due to timewalk, there is a small probability that the comparator will fire in the timeslot before the triggered timeslot, and the hit will be missed (see figure 8).

This demonstrates the importance of tuning the sampling time of the comparator after every threshold change during commissioning of a future tracker with CBC readout, in order to maximise efficiency. However, in the case of the H8 beam, which is asynchronous, this effect could be effectively eliminated by imposing tighter cuts on the trigger arrival time during the event selection.

4.3 Landau reconstruction

By selecting only those events where a one strip cluster would be expected (i.e. near the strip implant region), it is possible to eliminate the effect of efficiency reduction due to the loss of two strip clusters, and isolate the effect of increasing the threshold. This allows the reconstruction of the signal distribution.

Figure 9 shows the characteristic S-curve of efficiency as a function of threshold voltage, with selection of events with an interstrip position within 0.2 units of pitch of a strip implant. The distribution is assumed to be a Landau distribution of the following form,

$$L = \mathrm{e}^{-x-\mathrm{e}^{-x}}$$

where $x = (V_{CTH} - MPV)/\sigma$, MPV is the most probable value and σ is the spread of the distribution. The S-curve is then comes from the normalised reverse integral of this function,

$$y(x) = \frac{\int_{x}^{\infty} L\,\mathrm{d}x}{\int_{-\infty}^{\infty} L\,\mathrm{d}x}$$

The integral is calculated numerically, and fitted to the S-curve with a χ^2 minimisation. The best fit gives a most probable value of 771 mV and standard deviation of 20 mV. Figure 9 plots the best fit Landau (arbitrary units) and its integral $y(x)$ to the S-curve, and the χ^2 distribution of the two free parameters.

5 Conclusions

The CBC is designed for the readout of short strips in the CMS tracker at the HL-LHC. The simplicity of the binary design allows unsparsified output in the anticipated high luminosity environment and would allow the use of simple triggering algorithms on-detector for the first level trigger. A prototype CBC has been tested with a strip sensor in the 400 GeV H8 beamline at CERN, and performance was in agreement with expectations.

Spatial resolution is seen to be better than pitch / $\sqrt{12}$, due to the spatial distribution of one and two strip clusters. Large cluster (>4 strips) events are seen, and show consistency with delta ray production within the silicon sensor. Noise occupancy has been shown to be around the 10^{-4} at operating thresholds. Efficiency has been shown to depend on hit position across a strip, especially for high thresholds, where hits can be lost in the interstrip region due to charge sharing. However, this is not an issue around operating thresholds, where the measured efficiency is 98%, and could be improved further with better timing. Measurement of the characteristic efficiency in the near-strip region also reconstructs the sensor signal distribution.

Further iterations of the CBC are planned. The next is foreseen to have 256 channels for bump bonding to a hybrid, and include simple triggering logic, as required for the first level trigger at the HL-LHC [2, 9]. Performance and irradiation testing of prototype triggering modules for the outer tracking regions, utilising the next version CBC, will begin in 2013.

Acknowledgments

We gratefully acknowledge financial support from the U.K. Science and Technology Facilities Council. We thank the Imperial College High Energy Physics electronics and mechanical workshops, and also our UA9 collaborators for allowing parasitic operation in the test beam.

References

[1] M. Raymond et al., *The CMS tracker APV25 0.25 μm CMOS readout chip*, in 6th *LEB Workshop*, Cracow Poland (2000), CERN-LHCC-2000-041, CERN, Geneva Switzerland (2000).

[2] M. Raymond et al., *The CMS binary chip for microstrip tracker readout at the SLHC*, 2012 *JINST* **7** C01033.

[3] W. Scandale et al., *First results on the SPS beam collimation with bent crystals*, *Phys. Lett.* **B 692** (2010) 78.

[4] M. Pesaresi et al., *Design and performance of a high rate, high angular resolution beam telescope used for crystal channeling studies*, 2011 *JINST* **6** P04006.

[5] CMS collaboration, S. Chatrchyan et al., *The CMS experiment at the CERN LHC*, 2008 *JINST* **3** S08004.

[6] M. French et al., *Design and results from the APV25, a deep sub-micron CMOS front-end chip for the CMS tracker*, *Nucl. Instrum. Meth.* **A 466** (2008) 359.

[7] J. Varela, *CMS L1 trigger control system*, CERN-CMS-NOTE-2002-033, CERN, Geneva Switzerland (2002).

[8] G. Hall, *Ionisation energy losses of highly relativistic charged particles in this silicon layers*, *Nucl. Instrum. Meth.* **220** (1984) 356.

[9] D. Braga et al., *CBC2: a microstrip readout ASIC with coincidence logic for trigger primitives at HL-LHC*, submitted to *JINST* (2012).